

**SYNTHESIS AND CHARACTERISATION OF PURE AND Fe DOPED SnO₂
NANOPARTICLE VIA PRECIPITATION METHOD**

Project report submitted to
MES ASMABI COLLEGE
MSc. IN SCIENCE (PHYSICS)

Submitted by
FATHIMA FEBNA
REGISTER NO:

Under the guidance of
Dr. EBITHA EQBAL
Department of Physics
MES ASMABI COLLEGE
Vemballur-680671
Kerala, India



JUNE 2024

CERTIFICATE

This is to certify that the project work entitled “**SYNTHESIS AND CHARACTERISATION OF PURE AND Fe DOPED SnO₂ NANO PARTICLE VIA PRECIPITATION METHOD**” is done by **FATHIMA FEBNA A** is work done under the guidance of **Dr. EBITHA EQBAL**, Assistant Professor, Department of Physics, MES Asmabi college, in partial fulfilment of the requirement of the requirement for the award of the degree of master of science in physics.

HEAD OF THE DEPARTMENT

Dr.Ebitha Eqbal

Department of physics

DECLARATION

I FATHIMA FEBNA hereby declare that the project work entitled “**SYNTHESIS AND CHARACTERISATION OF PURE AND Fe DOPED SnO₂ NANO PARTICLE VIA PRECIPITAION METHOD**” submitted towards the partial fulfillment of the requirement for the fourth-semester course of MSc in science (physics), MES Asmabi college, is an original work written and composed entirely by me under the guidance of **Dr.EBITHA EQUBAL** Assistant Professor, Department of Physics, MES Asmabi college, P Vemballur-680671.

I also affirm that the information in this report is accurate to the best of my knowledge, and I have appropriately cited all external sources used.

Fathima Febna A

MSc physics

MES ASMABI College, Kodungallur

ACKNOWLEDGEMENT

I would like to express my deepest gratitude to my guide **Dr. EBITHA EQBAL**, Assistant professor of physics department, MES Asmabi college for her valuable guidance and insightful suggestions and great support for the successful completion of the project work that titled **“SYNTHESIS AND CHARACTERISATION OF PURE AND Fe DOPED SnO₂ NANO PARTICLE VIA PRECIPITATION METHOD IN ORDER TO STUDY ITS PROPERTIES”**. Their expertise in this topic greatly helps to know deeply about this topic and also helps to improve the quality of this project.

Also, I would like to express my sincere gratitude to our HOD *Dr. Sheena PA* and *Dr. A Biju*, the principle of MES Asmabi College, P Vemballur for the support and encouragement throughout this project.

I am also thankful to my *family, Teachers* and *friends* for their love and encouragement throughout this work.

Finally, I sincerely thank to my parents and everyone who has helped and encouraged me to make this project a reality.

ABSTRACT

Nanotechnology has become the most promising area of research with its tremendous application in the fields of science. In recent years, Tin oxide nanoparticles have gained significant attention due to their fascinating properties, particularly when synthesized in the nanometer range. Tin Oxide (SnO_2) is considered as a versatile metal oxide due to its various application such as gas sensing, photocatalysis, gas sensing etc. Various physical and chemical methods are used for the synthesis of doped and undoped tin oxide nano particle such as sol-gel method, precipitation method, combustion method, thermal spray pyrolysis etc. Out of this we select precipitation method. Precipitation method is a simple and lowcost method used for the synthesis of the nano particle. This project discussed the photocatalytic application of doped and undoped tin oxide nanoparticle prepared by precipitation method.

The prepared tin oxide nanoparticles were characterized using X-ray diffraction (XRD) analysis, UV-visible spectroscopy, and scanning electron microscopy (SEM). XRD method has been widely used to determine the crystal structure, lattice parameter, stresses, and crystallite size of the nanoparticles. XRD is a powerful, non-destructive characterization tool that provide essential information about various aspects of crystalline material. UV-Visible spectroscopy is widely used to characterize the nanoparticle. The UV-Visible Spectroscopy (UV-Vis Spectroscopy) technique measures the absorption of ultraviolet and visible light by a sample. SEM give the images of the sample in micrometer range by scanning the surface with focused beam of electron.

The optical band gap of the prepared tin oxide nanoparticle determined using the Tauc plot, gives the value 3.4 eV in the case of pure SnO_2 nano powder and 3.34 in the case of Fe doped SnO_2 nano powder. The XRD spectrum reveals that the prepared tin oxide nano powder has tetragonal structure, with an average crystallite size of approximately 12.5998nm for pure SnO_2 nano powder and 8.4972 for Fe doped SnO_2 nano powder. The calculated interplanar spacings from X-ray diffraction (XRD) data are as follows: 3.3498, 2.6460, 2.3690, 1.7644, 1.6748 and in the case of Fe doped SnO_2 it is found to be 3.3503, 2.6441, 2.3690, 1.7644, 1.6751. The strain and y-intercept calculated from the WH plot for pure SnO_2 nano powder is -0.00326 and 0.01202 and the grain size corresponding to this is 11.5442. The strain and y- intercept from WH plot in the case of Fe doped SnO_2 is -0.00435 and 0.01717 with corresponding grain size 8.0753. The SEM images of the prepared sample was taken in μm range. The SEM image of the pure Tin oxide nano particle shows that it has granular structure and homogeneous

structure for Fe doped Tin oxide nano particle. The photocatalytic activity of the pure Tin oxide (SnO_2) nano particle over the methyl orange dye was evaluated by monitoring the optical absorption spectra of methyl orange solution under direct sunlight and in the absence of sunlight. Prepared SnO_2 NPs exhibited an outstanding photocatalytic degradation of methyl orange within 48 hour.

LIST OF FIGURES

Fig.1.1. Schematic Diagram of Precipitation Method

Fig.1.2. Structure of SnO₂

Fig.2.1. Weighing Machine

Fig.2.2. Hot Air Oven

Fig.2.3. Muffle furnace

Fig.2.4. Schematic diagram of an X-ray tube

Fig.2.5. XRD instrument

Fig.2.6. Bragg's Diffraction

Fig.2.7. Schematic diagram of an X-ray diffractometer

Fig.2.8. Schematic diagram of SEM

Fig.2.9. FESEM instrument

Fig.2.10. UV spectrometer

Fig.3.1. XRD of the pure SnO₂ synthesized with calcination temperature 370°C

Fig.3.2. WH plot of pure SnO₂

Fig.3.3. Absorbance spectra of pure tin oxide nanoparticles prepared by precipitation method.

Fig.3.4. Optical bandgap of the pure tin oxide nanoparticles synthesized by precipitation

Method

Fig.3.5. SEM image of pure SnO₂ synthesised by precipitation method

Figure.3.6. Photocatalytic degradation of methyl orange dye under the irradiation of direct sunlight using SnO₂ NPs

Figure.3.7. Methyl orange solution with SnO₂ NPs after 24 hours and after 48 hours placed under irradiation of direct sunlight

Figure.3.8. Photocatalytic degradation of methyl orange dye in absence of sunlight using SnO₂ NPs

Fig.3.9. XRD of the Fe doped SnO₂ synthesized with calcination temperature 370°C

Fig.3.10. To calculate crystalline size and strain of Fe doped SnO₂ from XRD data using Williamson-Hall (W-H) plot method

Fig.3.11. Absorbance spectra of Fe doped tin oxide nanoparticles synthesized by precipitation method

Fig.3.12. Optical bandgap Fe doped tin oxide nanoparticles synthesized by precipitation method

Fig.3.13. SEM image of Fe doped SnO₂ synthesised using precipitation method.

LIST OF TABLES

Table 3.1. Crystalline size of SnO₂ calculated using Debye Scherrer's Equation

Table 3.2 d spacing of SnO₂ calculated using Bragg's equation.

Table 3.3 values of $\beta \cos\theta$ and $4 \sin \theta$.

Table 3.4 Grain size comparison data from Debye Scherrer's formula and W-H plot

Table 3.5 Texture coefficient of each (hkl) plane.

Table 3.6. Crystalline size of Fe doped SnO₂ calculated using Debye Scherrer's Equation

Table 3.7 d spacing of Fe doped SnO₂ calculated using Bragg's equation.

Table 3.8 values of $\beta \cos\theta$ and $4 \sin \theta$ for Fe doped SnO₂.

Table 3.9 Grain size comparison data from Debye Scherrer's formula and W-H plot of Fe doped SnO₂

Table 3.10 Texture coefficient of each (hkl) plane.

CONTENTS

CHAPTER 1:Introduction

- 1.1.Nanotechnology
- 1.2.Tin Oxide (SnO_2) properties and structure
- 1.3. Synthesis Techniques
- 1.4. SnO_2 properties and structure
- 1.5. Application
 - 1.5.1. Photocatalytic Application
 - 1.5.2. Gas Sensing
 - 1.5.3. Lithium Batteries

CHAPTER 2:Experimental and Characteristic techniques

- 2.1. Experimental
 - 2.1.1. Powder preparation
- 2.2. Photo catalytic action of pure and Fe doped SnO_2
 - 2.2.1. Procedure
- 2.3. Characteristic Technique Used
 - 2.2.1.X-Ray Diffraction

2.2.2. Scanning Electron Microscopy

2.2.3. Ultraviolet – Visible spectroscopy

CHAPTER 3: Result and Discussion

3.1. Synthesis of pure SnO₂

3.1.1. XRD analysis

3.1.1(a). Crystalline Size

3.1.1(b). d spacing or Interplanar Spacing

3.1.1(c). WH plot

3.1.2. UV-VIS Spectroscopic Analysis

3.1.3. SEM

3.1.4. UV- VIS spectroscopy of Photocatalytic action

3.2. Synthesis of Fe doped SnO₂

3.2.1. XRD analysis

3.2.1(a). Crystalline Size

3.2.1(b). d spacing or Interplanar Spacing

3.2.1(c). WH plot

3.2.2.UV-VIS Spectroscopic Analysis

3.2.3.SEM

3.2.4.UV- VIS spectroscopy of Photocatalytic action.

3.3. Conclusion

3.4.Future Scope Of SnO₂ nano particles

CHAPTER 1:Introduction

1.1 Nanotechnology

1.2 Tin Oxide(SnO₂) nano particle

1.3 Synthesis Techniques

1.4 SnO₂ Properties and Structure

1.5 Application

1.5.1 Photocatalytic Application

1.5.2 Gas Sensing

1.5.3 Lithium Batteries

INTRODUCTION

1.1.Nanotechnology

Nanotechnology has emerged as a highly promising field of research, with significant applications across various scientific domains. Its considerable amount of recognition is due to their distinctive electrical, physical, chemical, and magnetic properties. Nanotechnology involves designing and manipulating structures at the atomic or molecular scale, with at least one dimension measured in nanometers. These tiny structures exhibit unique properties due to their size, leading to advancements in various fields.

At nanoscale, the laws of physics operate in an unfamiliar way because of two important reasons: high surface-to-volume ratio and quantum effect. A material's characteristics at smaller scales can differ greatly from those at larger ones when a particle with size of roughly 1-100 nanometers is formed. The behavior and properties of the particle can be governed by the quantum effect at this small scale. The concept of "tunability" in a property is a surprising outcome of quantum processes at the nanoscale.

That is achieved by changing the size of the particle. At the nano scale, altering the size of the particle can lead to change in properties including the melting point, fluorescence, electrical conductivity, magnetic permeability, and chemical reactivity can change as the function of the size of the particle.

Another important attribute of the nanoscale material is the large surface to volume ratio. The substantial surface area-to-volume ratio and minuscule dimension of these materials can lead to novel or improved electrical, optical, magnetic, catalytic, and antimicrobial characteristics compared to large scale counterparts. An important consequence of each of these properties is that they offer novel methods for tuning the properties of materials and devices.

Nanotechnology offers unparalleled insights into materials and devices, with the potential to revolutionize various fields. By manipulating structures at the nanoscale as a controllable physical parameter, we can significantly enhance the performance of existing chemicals and materials. In recent years, tin oxide has garnered significant interest owing to its captivating characteristics, further enhanced through the fabrication of this substance at the nanoscale level. The widespread interest in Tin oxide nanoparticles stems from their adaptability, with uses extending to optoelectronic device, solid state gas sensors, electrodes for lithium-ion batteries, field emission displays etc.

1.3. Tin Oxide (SnO₂) nanoparticle

Tin oxide is an n-type semiconductor with a wide bandgap of 3.6 eV. Tin oxide is a transparent conducting oxide material with high transparency and high electrical conductivity. So it is used in optoelectronic devices and solar cells. Tin oxide is chemically and thermally stable at varying temperatures, it is used as a favorable option for various gas sensing devices.

Tin oxide nano powder is a nontoxic substance, so it is widely used in the cosmetic industry. It has high IR radiation reflectivity and is used in heat reflecting windows and mirrors. It is used for dye sensitizing purposes, in liquid crystal displays, in humidity sensor. Various techniques are utilized for the synthesis SnO₂ nanoparticles. They are combustion method, co-precipitation technique, ball milling, chemical precipitation, thermal spray pyrolysis, sol-gel method etc. Tin oxides prepared by these methods have many applications in different fields.

1.4.Synthesis Method

Precipitation Method:

Tin oxide nanoparticles can be synthesized using various methods. They are combustion method, co-precipitation technique, ball milling, chemical precipitation, thermal spray pyrolysis, sol-gel method etc. Out of this we select precipitation method. Precipitation method is a simple and low cost technique for synthesizing nanoparticles. One of the most commonly employed manufacturing techniques for nanomaterials involves the precipitation of solids from a solution containing metal ions. This method can yield both metallic nanoparticles and non-oxides or metal oxides. The process relies on how salts interact with solvents. By introducing a precipitating agent, the desired particle precipitation occurs, followed by filtration and thermal post-treatment. Reaction kinetics play a crucial role in determining particle size, size distribution, crystallinity, and morphology during precipitation processes. Additionally, factors such as source material concentration, temperature, order of material addition, basicity and mixing procedures influence the outcome.

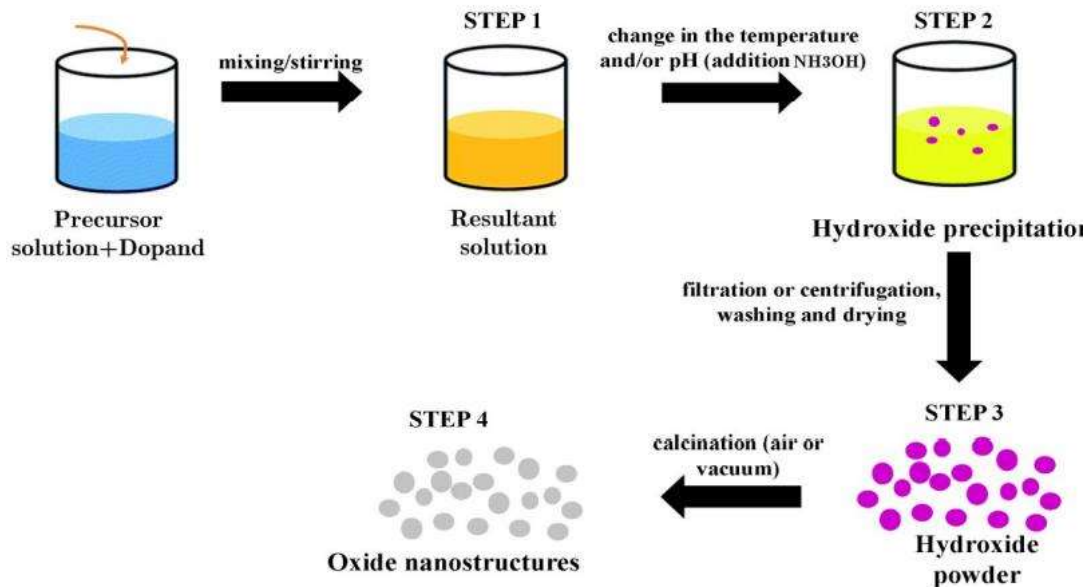


Fig.1.1.Schematic Representation of Precipitation Method

1.5.SnO₂ Properties and Structure

Tin oxide is a n type semiconductor, also known as stannic oxide with chemical formula SnO₂ has received a tremendous attention in semiconductor field due its unpredictable application in various fields such as energy saving coatings, gas sensors, photocatalysis, biosensors, textile industry etc. Tin oxide, specifically a transparent conducting oxide material known for its high transparency and excellent electrical conductivity. It is considered a versatile metal oxide due to its variable valence states and the presence of oxygen vacancies. Structurally, SnO₂ adopts a tetragonal crystal lattice, with hexacoordinated tin ions and tri-coordinated oxygen atoms. Its molar mass is approximately 150.71 g/mol .SnO₂ exist in two forms in nature with two oxidation states +2 and +4. It has melting point of 1630 °C and a boiling point of 1900°C. It has density of 6.95 g/cm³.

Tin dioxide (SnO₂), an n-type wide bandgap semiconductor with a bandgap of 3.6 eV at 300 K, has garnered significant attention due to its high carrier density, oxygen vacancies, chemical stability, and exceptional electrical, optical, and electrochemical properties. These properties make SnO₂ suitable for a wide range of applications, including solar cells, catalytic support materials, transparent electrodes, and solid-state chemical sensors. This bandgap is particularly appropriate for catalysis, gas sensors, transparent electrodes, Li-ion batteries, and so on. It is a oxygen deficient n type semiconductor. It is also called the stannic oxide. SnO₂ is insoluble in water. It is amphoteric, dissolving base and acids.

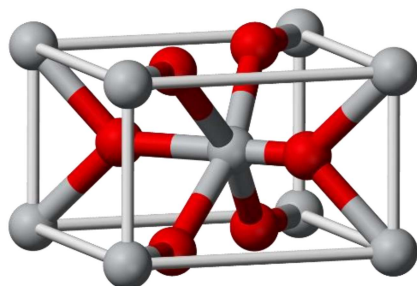


Figure.1.2. structure of SnO₂

1.6.Applications

SnO₂ has been largely investigated and used due its varieties of applications such as photocatalysis, gas sensing, lithium ion batteries etc. The application mainly depends on their morphologies and special assemblies of nanomaterials.

1.6.1. Photocatalytic

SnO₂ nano particle has significant application in catalysis due its unique properties. Tin oxide nanomaterials exhibit strong catalytic activity in the degradation of the organic pollutants in solutions because of their wonderful properties such as low cost , transparency, high photosensitivity, photostability etc. The photocatalytic application of SnO₂ nanoparticle were investigated via methyl orange as a model organic compound under UV light irradiation. The study shows that, SnO₂ is efficient catalysis in removing organic pollutant in water.

1.6.2. Gas sensing

SnO₂ has been extensively investigated and used to detect variety of gases for practical applications. SnO₂ materials with different morphology and structure have been fabricated in recent years in order to improve the gas sensing technology. Tin oxide is the most common used gas sensing material. Its Gas sensing technology has garnered significant interest in practical applications, spanning both industrial and academic domains. The gas sensing means discriminating and monitoring the concentration of gases in the industrial processes as well as in everyday life. Due to high demand for reliable and robust gas sensing devices, academic research play important rule for improving the capability to detect the gas species. excellent electrical and optical property makes SnO₂ as suitable for gas sensing.

1.6.3. lithium batteries

SnO₂ Nanomaterials are versatile device due to its momentous application in various field including lithium-ion batteries. Lithium-ion batteries (LIBs) are the most advanced electrochemical energy-storage technology for mobile and consumer applications, boasting energy and power densities significantly

higher than other battery systems The electrolyte carries positively charged ions from the anode to cathode and vice versa through the separator. Lithium-ion batteries are used in many product such as electronics, toys, wireless headphones, hand held power tools, electric vehicles and electrical energy storage systems.

CHAPTER 2

2.1. Experimental

2.1.1. Powder preparation

2.2. Photo catalytic action of pure and Fe doped SnO₂

2.2.1.Procedure

2.3. Characteristic Technique Used

2.2.1.X-Ray Diffraction

2.2.2.Scanning Electron Microscopy

2.2.3. Ultraviolet – Visible spectroscopy

2.1.Experimental

2.1.1. Powder preparation

For the powder preparation first step is to clean the beakers, spatula and glass rod using distilled water and acetone. Before using the weighing machine, switch it on and allow it to stabilize for at least 5 to 15 minutes. For the weighing first we clean the spatula with acetone and use the cleaned spatula to take the salt from its bottle. Also clean the weighing machine with acetone and ensure it is calibrated in to zero and place a piece of butter paper on the weighing machine. Then add the salt to the butter paper and weigh it accordingly. To make the SnO₂ nano powder, we have to take 1.12g (0.125 molar) stannous chloride dihydrate (SnCl₂.2H₂O) dissolved in 20 ml of distilled water. We have to add .1 g of CTAB dissolved in 20 ml of distilled water in to solution of stannous chloride. Then allow it for magnetic

stirring for 15minute. The Ammonium hydroxide solution was gradually added dropwise to the prepared tin chloride solution while constantly stirring, as precipitating agent and controlling solution pH. With the addition of Ammonium hydroxide solution, precipitate was formed in the solution, and the pH value reached to 10. As the solution pH was maintained, further stirring was stopped, and the precipitate was dried by putting in oven at 300°C for 4 hours. After heating put it in muffle furnace for calcination. After that a solid matter was obtained which was well grinded into powder and put in a bottle. This desired product which was further investigated by different characterization techniques.

For making Fe doped SnO₂ nano powder, 4.28g of stannous chloride dihydrate dissolved in 20ml of distilled water and 0.911g of CTAB added to the solution of SnO₂.2H₂O. Take 0.1622g of FeCl₂ and dissolve it in 20 ml of distilled water in another beaker and allow the both solution for magnetic stirring foe 5 minute separately. Then mix both solution and allow it for magnetic stirring for 15minute. Ammonium hydroxide is added to the solution dropwise while stirring continuously to keep the pH of the mixture at 8. As the pH of the solution was maintained, further stirring was stopped, and the precipitate was dried by putting in oven at 300°C for 4 hours. After heating put it in muffle furnace for calcination. After that a solid matter was obtained which was well grinded into powder and put in a bottle.



Fig.2.1. Weighing balance



Fig.2.2. Hot air Oven



Figure.2.3.Muffle Furnace

2.2. Photo catalytic action of pure and Fe doped SnO₂ nano powder

The uncontrolled discharge of harmful chemicals, dangerous textile dyes, and pesticides from different industries into waterways has led to significant environmental issues. Excessive impurities in water harm both animals and humans, and certain colored chemicals can cause illness. Therefore, it is crucial to treat water containing poisonous chemicals before disposing of it into the environment to reduce environmental pollution. New research has shown that nanostructured semiconductor metal oxide are great at cleaning up different water pollutants. SnO₂, one of these metal oxides, is widely used to get rid of textile dyes and other organic substances because it's stable, reactive on surfaces, good for photocatalysis, cheap, and not very toxic. synthesized SnO₂ nanoparticles effectively served as a catalyst in degrading methyl orange (MO) dye. The photocatalytic activity of the nanoparticles was investigated at different calcination temperatures, and the results indicated that the SnO₂ nanoparticles. Here we evaluate the photo degradation of methyl orange in the presence of the SnO₂ catalyst in the presence and absence of sun light for 24 and 48 hours to calculate the absorption percentage.

2.2.1.Procedure

To analyze the photo catalytic action of pure and Fe doped SnO₂ we need 2 cleaned beaker and a spatula. Label two beakers for pure SnO₂. Add 30 ml of distilled water to each beaker. Add 30 ml of distilled water to each beaker and Add a drop of methyl orange to each beaker. Take 0.001g of pure

SnO₂ nano powder and add it to the appropriate beaker. Cover the two beaker and place one beakers (one with pure SnO₂) in light for 24 hours. Keep the next one in a dark place. After 24 hours, take UV spectroscopy measurements of the solutions in beakers. Repeat the UV spectroscopy measurements after 48 hours and calculate the rate of degradation from the absorption spectra.

2.2.Characterisation Technique Used

2.2.1.X-Ray Diffraction

Wilhelm Conrad Röntgen made the groundbreaking discovery of X-rays in 1895. X-rays are a type of high-energy electromagnetic radiation. They occupy a region in the electromagnetic spectrum between ultraviolet (UV) rays and gamma rays. Unlike visible light, X-rays have higher energy and can penetrate many solid substances, including living tissue. X-rays, being uncharged or neutral particles, travel in straight lines at the speed of light. They cannot be deflected by electric fields, but they may be influenced by magnetic fields. X-rays have several interesting properties: they can affect photographic film, produce fluorescence, and cause photoelectric emission. Additionally, they exhibit varying penetration power in different materials, with higher-density substances offering the least penetration. X-rays are generated in evacuated glass tubes, where a heated filament emits electrons. These accelerated electrons collide with a metal target, resulting in the production of X-ray radiation through the conversion of kinetic energy into heat.

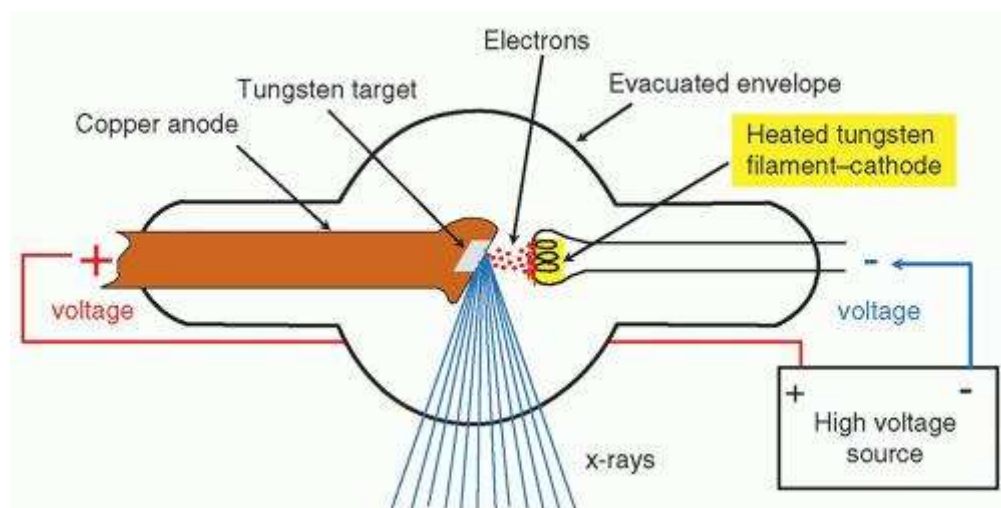


Figure 2.4. schematic diagram of an x-ray tube

Diffraction occurs when waves, such as light or sound, bend around obstacles or spread out when passing through narrow openings. In the context of X-ray diffraction (XRD). In XRD, a coherent X-ray wave encounters the atoms within a crystal lattice. These atoms act as tiny scatterers, causing the X-rays to deviate from their original path. The scattered X-rays interfere with each other, leading to a diffraction pattern. The scattered X-rays interfere with each other, leading to a diffraction pattern. The scattered X-rays interfere with each other, leading to a diffraction pattern. Crystals have a repeating, ordered arrangement of atoms. This periodicity allows the scattered X-rays to constructively or destructively interfere. The resulting diffraction pattern contains valuable information about the atomic arrangement within the crystal. When X-rays strike a crystal, they scatter in specific directions due to the crystal's lattice structure. The angles and intensities of these scattered X-rays form a characteristic diffraction pattern. By analyzing this pattern, scientists can determine the crystal's unit cell dimensions, symmetry, and atomic positions. Amorphous materials, such as glass, lack a periodic array with long-range order. Unlike crystalline materials, they do not produce a diffraction pattern when exposed to X-rays. Instead, their atomic arrangement resembles a disordered network, resulting in a diffuse scattering of X-rays.

On the other hand, the X-ray diffraction (XRD) method has been widely used to determine the crystal structure, lattice parameters, stresses, and crystallite size of nanoparticles. XRD is a valuable, non-destructive characterization tool that offers essential details about various aspects of crystalline substances. With the use of these methods, it is possible to determine how an X-ray beam's scattered intensity changes with incident and scattered angles, polarization, and wavelength or energy. Based on the elastic scattering of X-rays from the individual atoms' electron clouds, XRD provides information about the atomic structure of materials. XRD reveals the different phases present in a material. It aids in identifying a substance's crystal structure. In X-ray crystallography (XRD), a specimen is exposed to a monochromatic beam of X-rays with a typical wavelength ranging from 0.7 to 2 Å. If Bragg's law is satisfied, the X-rays are diffracted by the crystalline phases in the specimen.

$$n\lambda = 2d \sin\theta$$

d -interplanar distance

λ - wavelength of X-ray

θ -diffraction angle

$n=0,1,2,3,\dots$

n is the order of diffraction



Figure 2.5. xrd instrument

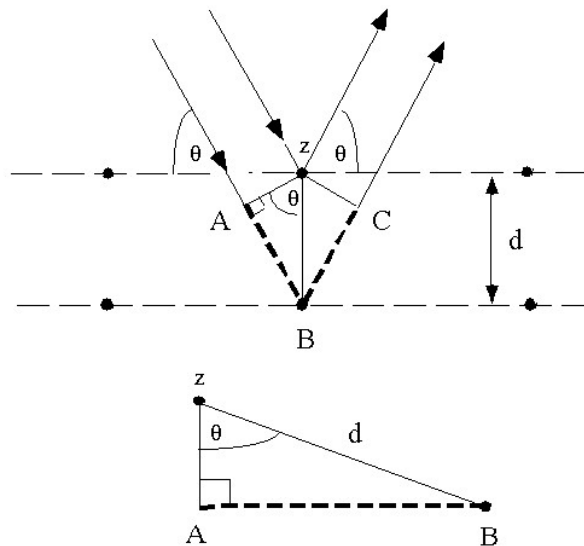


Figure 2.6. Braggs Diffraction

The intensity of the diffracted X-rays is carefully measured as a function of the diffraction angle (2θ) and the orientation of the specimen. XRD is a nondestructive technique that does not require elaborate sample preparation.

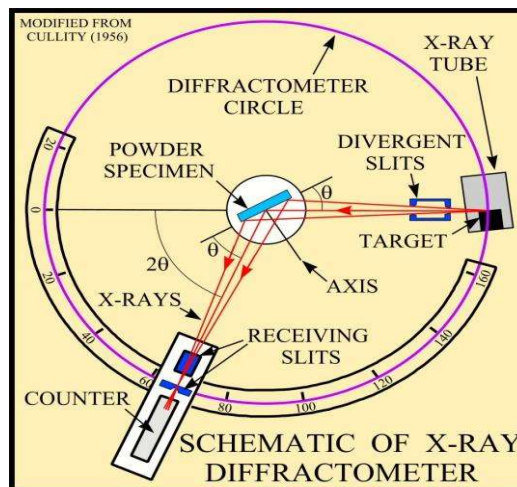


Figure.2.7 Schematic diagram of X-ray Diffractometer

The main components of an X-ray diffractometer include the X-ray tube (the source of X-rays), incident-beam optics (which condition the X-ray beam before it hits the sample), the goniometer (which holds and moves the sample, optics, detector, and/or tube), the sample holder (used to fix the sample, depending on its state), receiving-side optics (which condition the X-ray beam after it encounters the sample), and the detector (which counts the number of X-rays scattered by the sample).

x-ray diffraction (XRD) patterns provide valuable insights into various aspects of materials.

- **Phase Composition: Quantitative Phase Analysis:** By comparing peak intensities, XRD helps determine the relative amounts of different phases in a mixture. This is crucial for identifying the composition of complex samples.
- **Unit Cell Lattice Parameters and Bravais Lattice Symmetry:** XRD reveals the periodic arrangement of atoms in a crystal lattice. By analyzing diffraction peaks, we

can extract information about the unit cell dimensions (such as lattice constants) and the symmetry of the lattice.

- **Crystal Structure:** XRD patterns can be refined using the Rietveld method, which involves fitting the entire diffraction pattern to a theoretical model. This yields precise crystallographic information, including atomic positions and thermal vibrations.
- **Epitaxy:** XRD characterizes the alignment of crystal layers in epitaxial thin films.
- **Crystallite Size and Micro strains**

In practice, diffraction from a crystal specimen results in a peak with a certain width, known as peak broadening. This phenomenon occurs because the ideal Bragg diffraction peak, which would be a sharp line, is affected by factors such as crystal size.

The Debye-Scherrer formula provides a way to estimate the average crystallite size based on this peak broadening.

$$D = \frac{0.9 \lambda}{\beta \cos \theta}$$

D – crystallite size

λ – wave length(1.54Å)

β - Full maxima half width

θ - Diffraction angle

It assumes that lattice deformation is negligible and relates the crystalline size (D) to the X-ray wavelength (λ), the full width at half maximum (FWHM) of the diffraction peak (β), and the angle of diffraction (θ). By analyzing the FWHM, scientists gain insights into the crystal structure and properties

2.2.SCANNING ELECTRON MICROSCOPY(SEM)

A Scanning Electron Microscope is type of electron microscope that scan the surface of the microorganisms using a beam of low energy electron to focus and examine specimen. SEM uses high energy electron beam to generate variety of signal at the surface of the solid specimen. The interaction of electron with specimens atoms generate signal such as secondary electrons(SEs), backscattered electrons(BSEs), Auger electrons, characteristic x-ray ,etc. These signals reveal details about the sample's external morphology (such as texture), chemical composition, and the crystalline structure and orientation of the materials comprising the sample.

The Scanning electron microscope works on the principle that the interaction of primary electron with a specimen's atom generate several electrons. These electrons are secondary electrons, backscattered electrons, and diffracted backscattered electrons which are used to view crystallized elements and photons Secondary and backscattered electrons are used to produce an image. Most of the electron scattered instead of being transmitted when they interact with positively charged nucleus This elastically scattered electrons are called Base Scattered Electrons(BSEs).Some of the electrons are scattered inelastically due to the loss in kinetic energy when it interact with the orbital shell electrons . These electrons are called the secondary electrons(SEs). The secondary electrons, emitted from the specimen, primarily contribute to detecting the morphology and topography of the specimen. In contrast, the backscattered electrons reveal variations in the composition of the specimen's elements.

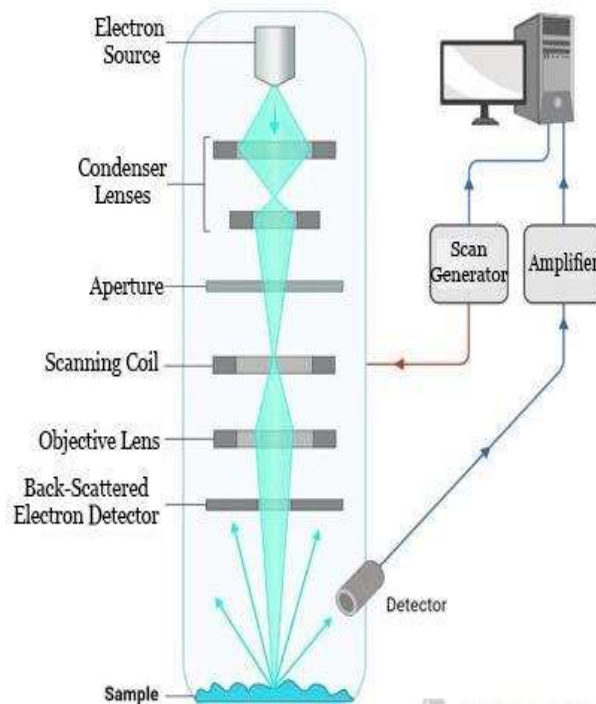


Figure.2.8. schematic diagram of SEM

The lateral spatial resolution of a SEM image is affected by the size of the volume from where the signal electrons escape. Images formed by secondary electrons (SEs) exhibit better spatial resolution than those formed by backscattered electrons (BSEs) in a Scanning Electron Microscope (SEM). They have better spatial resolution because they originate from a shallow depth within the material. Due to their low escape depth, SEs provide high-resolution surface information. SEM images are commonly used for topographical imaging and surface characterization.

A typical SEM has an image resolution of 5–10 nm, but a modern state SEM like field emission SEM is capable of providing an image resolution of 1nm. This resolution allows researchers to visualize surface features and structures at a relatively coarse level.



Figure.2.9.FESEM instrument

2.3.Ultraviolet- Visible spectroscopy

Ultraviolet-Visible Spectroscopy (UV-Vis Spectroscopy) is indeed a powerful analytical technique used to study the interaction of light with matter. The UV-Visible Spectroscopy (UV-Vis Spectroscopy) technique measures the absorption of ultraviolet and visible light by a sample. It operates based on Beer-Lambert's law, which states that the sample's absorbance is directly proportional to its concentration and the path length of the sample.

$$I(\lambda) = I_0(\lambda) e^{-\alpha(\lambda)t}$$

Where, $I(\lambda)$ = Intensity of Transmitted Light. This represents the amount of light that passes through the sample at a specific wavelength (λ). It's the light intensity observed after it has interacted with the sample.

$I_0(\lambda)$ = Initial Intensity of Incident Light . This is the intensity of light before it enters the sample. It serves as a reference point to measure how much light is absorbed by the sample.

$\alpha(\lambda)$ = Absorption Coefficient. The molar absorptivity (or molar extinction coefficient) quantifies the strength with which a substance absorbs light at a specific wavelength. It depends on the nature of the sample and the wavelength of light.

t = Sample Path Length. This refers to the distance the light travels through the sample. It's usually measured in centimeters (cm) and represents the thickness of the sample.



Figure 2.10. UV visible spectrometer

When light passes through the sample, its intensity decreases due to absorption by the sample. The exponential term accounts for this attenuation. As the concentration of the absorbing species increases, more light is absorbed, resulting in a higher absorbance (A). The relationship is linear for dilute solutions, allowing us to quantify the concentration of a substance based on its absorbance

CHAPTER 3

Results and Discussion

3.1.Synthesis of pure SnO₂

3.1.1.XRD analysis

3.1.1(a). Crystalline Size

3.1.1(b). d spacing or Interplanar Spacing

3.1.1(c). WH plot

3.1.2.UV-VIS Spectroscopic Analysis

3.1.3.SEM

3.1.4.UV- VIS spectroscopy of Photocatalytic action

3.2.Synthesis of Fe doped SnO₂

3.2.1.XRD analysis

3.2.1(a). Crystalline Size

3.2.1(b). d spacing or Interplanar Spacing

3.2.1(c). WH plot

3.2.2.UV-VIS Spectroscopic Analysis

3.2.3.SEM

3.2.4.UV- VIS spectroscopy of Photocatalytic action.

3.3. Conclusion

3.4. References

3.1.Synthesis of pure SnO2

3.1.1.XRD Analysis

The X-ray diffraction pattern of the SnO2 nanoparticle synthesized by precipitation method is shown in figure. X-ray diffraction (XRD) is commonly employed to investigate the crystallography of a sample by analyzing the diffraction patterns produced when X-rays interact with a crystalline material, researchers can determine details such as lattice structures, crystal phases, and interplanar spacing, optical properties, crystalline size and morphology. It's a powerful technique for understanding the arrangement of atoms within solids. The Debye-Scherrer formula yields the average size of the particle (D), which can be found by,

$$D = \frac{0.9 \lambda}{\beta \cos \theta} \dots\dots\dots 1$$

D= Crystalline Size

θ =Glancing

λ = Wave length of the X-ray radiation

β = full width at half maximum to the diffraction peak.

The figure.3.1 shows the XRD pattern of the pure SnO2 synthesized at calcination temperature 370°C.The peaks at 2θ value 26.607°, 33.8°, 37.9°, 51.8°and 54.7° correspond to the crystallographic planes (110), (101), (200), (211), and (220), respectively. All the peaks in XRD were matched with the diffraction data of the tetragonal structure of tin oxide. The spectra were plotted using the origin lab 2018. The particle size found using the Debye–Scherrer Formula. The average size of the particle is to found be 12.5998 nm, JCPDS card No.00-210-4754 and unit cell parameters a =4.7358 Å and c = 3.1873 Å.

The spectra are shown below.

For calcination temperature 370 °C:-

The average particle size is found to be 12.5998 nm

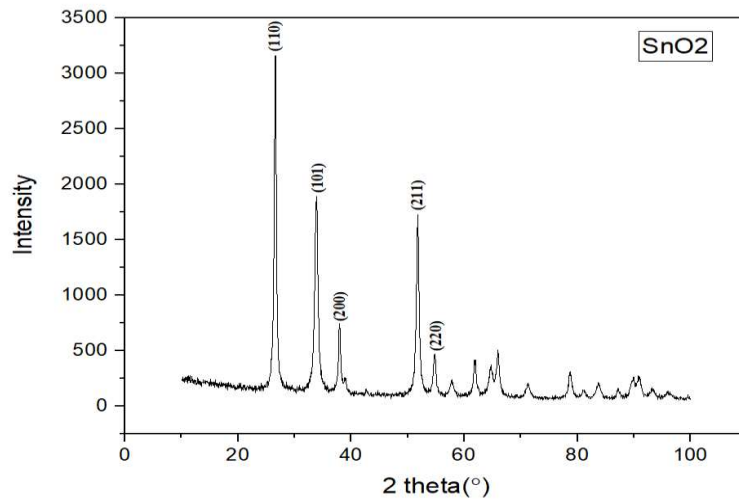


Figure.3. XRD of the pure SnO₂ synthesized with calcination temperature 370°C

3.1.1(a). Crystalline size

To calculate the crystalline size and average crystalline size from the XRD data, we can use the Scherrer equation. The Scherrer equation is limited to **nano-scale crystallites**. We can calculate average crystalline based on XRD data using the Scherrer equation.

$$D = \frac{K \lambda}{\beta \cos\theta} \quad (2)$$

where,

D = crystalline size (nm)

K = 0.9 Scherrer size (nm)

λ = 0.15418 nm (wavelength of the X-ray source)

β = FWHM (radians)

θ = peak position (radians)

XRD peaks Position 2θ (deg)	FWHM (β)	Bragg's peaks	Crystalline size D (nm)	Average crystalline size D (nm)
26.58	0.5444	1 1 0	14.7427	12.5998
33.84	0.7329	1 0 1	10.3697	
51.77	0.6237	2 1 1	11.4588	
54.76	0.5101	2 2 0	13.8279	

Table 3.1 Crystalline Size of pure SnO₂ calculated using Debye Scherrer's Equation

3.1.1(b).d interplanar spacing

Interplanar spacing or d spacing from the XRD data can be calculated using the Bragg's equation is given by,

$$n \lambda = 2d \sin \theta \quad (3)$$

or,

$$d = \frac{n\lambda}{2 \sin \theta} \quad (4)$$

Where,

$\lambda = 1.5418 \text{ \AA}$ (wavelength of incident X- ray)

θ = peak position (in radians)

$n = 1$ (order of diffraction)

d = interplanar spacing or d spacing (in \AA)

2 theta	theta	d-spacing
26.588	13.2942	3.3498
33.8488	16.9244	2.6460
37.9500	18.9750	2.3690
51.771	25.8855	1.7644
54.7634	27.3817	1.6748
		This is our desire value in \AA

Table 3.2 *d* spacing of pure SnO₂ calculated using Bragg's equation.

3.1.1.(c) WH Plot

X-ray peak broadening analysis was employed to assess **crystalline sizes** and lattice strain using the Williamson-Hall (W-H) analysis. In our study, we utilized W-H analysis to estimate crystallite size and lattice strain. In X-ray diffraction (XRD) data, the broadening of the peaks (β_T) results from the combined effects of crystallite sizes (β_D) and micro strain (β_ϵ).

Total broadening = Broadening due to crystallite sizes + Broadening due to strain

$$\beta_T = \beta_D + \beta_\epsilon \quad (5)$$

Where β_T represents the total peak broadening, β_D corresponds to the contribution from crystallite size effects, β_ϵ accounts for the impact of micro strain. The crystalline size D which is the average grain size is estimated using the Scherrer's formula

$$D = \frac{K\lambda}{\beta_D \cos \theta} \quad (6)$$

or

$$\beta_D = \frac{K\lambda}{D \cos \theta}$$

Where, β_D represents the full width at half maximum (FWHM) of the peak in radians

$K=0.9$ is the shape factor

λ = wavelength of the x-ray used

D =Crystalline size in nm

θ =peak position in radians.

Similarly, the XRD peak broadening due to micro strain is given by,

$$\beta_\epsilon = 2 \epsilon \tan\theta \quad (7)$$

where β_ε is broadening due to strain, ε is the strain and θ is the peak position in radians.

Substituting (6) and (7) in equation (5) we obtain,

$$\beta_T = \frac{K\lambda}{D \cos\theta} + 4\varepsilon \tan \theta \quad (8)$$

or

$$\beta_T = \frac{K\lambda}{D \cos\theta} + \frac{4\varepsilon \sin\theta}{\cos\theta}$$

Multiplying both sides by $\cos \theta$ we obtain,

$$\beta_T \cos \theta = \frac{K \lambda}{D} + 2 \varepsilon \sin \theta$$

or

$$\beta_T \cos \theta = 2\varepsilon \sin \theta + \frac{K\lambda}{D} \quad (9)$$

Equation (9) represents a straight line, in which ε is the gradient (slope) of the line and $\frac{K\lambda}{D}$ is the y-intercept.

We have the standard equation of a straight line

$$y = mx + c \quad (10)$$

where m represents the slope of the line and c is the y-intercept.

Comparing equation (9) with equation (10) we have,

$$y = \beta_T \cos \theta \quad (i)$$

$$m = \varepsilon \quad (ii)$$

$$x = 4 \sin \theta \quad (iii)$$

$$c = \frac{K\lambda}{D} \quad (iv)$$

Where the value of m represents slope of the line which correspond to be the value of strain “ε” and y-intercept ‘c’ corresponds to “ $\frac{k\lambda}{D}$ ”

theta (degree)	theta (radians)	FWHM (degree)	FWHM (radians)	$\beta \cos\theta$	$2 \sin \theta$
26.5884	0.23202	0.52442	0.009152856	0.008908	0.459903
33.8490	0.29538	0.73292	0.012791867	0.012238	0.582223
51.7710	0.45178	0.62373	0.010886142	0.009794	0.873149
54.7647	0.47791	0.51014	0.008903623	0.007906	0.919853

Table 3.3 values of $\beta \cos\theta$ and $4 \sin \theta$.

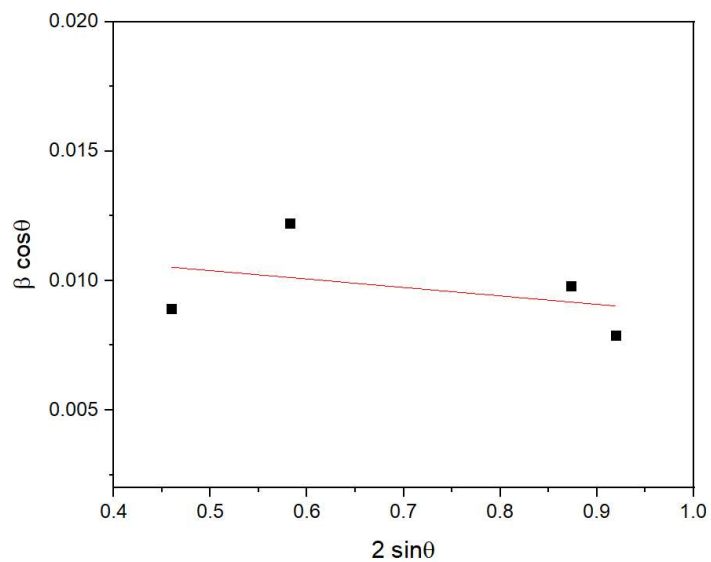


Fig 3.2 WH plot of pure SnO2

Slope of the plot is the strain. So the value of strain (ϵ) = -0.00326

The value of y-intercept “c” = 0.01202

$$\text{y-intercept } c = \frac{k\lambda}{D}$$

Or

$$D = \frac{k \lambda}{C}$$

Where $k = 0.9$ is the shape factor and $\lambda = 0.15418\text{nm}$ is the wavelength of the X-ray source, putting all these values we get,

$$D = 11.5442 \text{ nm}$$

The dislocation density is defined as the length of dislocation lines per unit volume is calculated from the crystalline size D using equation

$$\delta = \frac{1}{D^2}$$

Dislocation density is used to determine length of dislocation lines per unit volume.

In the case of pure SnO_2 the Dislocation calculated from the grain size is shown below,

Grain Size (D) from the Scherrer's formula (nm)	Dislocation density ($\times 10^{15}$) (lines/m ²)	Grain size (D) from the W-H plot (nm)	Lattice strain
12.5889	6.30	11.5442	-0.00326

Table.3.4 Grain size comparison data from Debye Scherrer's formula and W-H plot

W-H plot for the samples possess negative slope which is due to lattice compression. The reflection intensity for the each peak in the XRD data contains information about the preferential or random growth of polycrystalline thin films, which is investigated by calculating the texture coefficient $\text{TC}(hkl)$ for the plane using the following equation:

$$\text{TC}(hkl) = \frac{I(hkl)}{\frac{1}{N} \sum I(hkl)}$$

Where $TC(hkl)$ is the texture coefficient of hkl plane, $I(hkl)$ represents the intensity of the diffraction peak corresponding to the crystallographic plane (hkl) . and N is the number of reflections. Table 3.5 shows texture coefficient of each (hkl) plane. The texture coefficient provides insights into the preferential or random growth of the thin film along specific crystallographic directions. A high TC value indicates strong preferential orientation, while a low value suggests random orientation of the grains in the film. From the table 3.5, (110) has a high preferred orientation, as can be seen.

hkl value	TC of pure SnO ₂
1 1 0	1.53
1 0 1	1.139
2 0 0	0.98
2 1 1	0.33

Table 3.5 Texture coefficient of each (hkl) plane

3.1.2.UV-VIS Spectroscopic Analysis

The UV-VIS spectroscopy was done at room temperature with in wavelength range 200nm-800nm. The Absorption spectrum of pure SnO₂ synthesized by precipitation method at calcination temperature 370°C is given below.

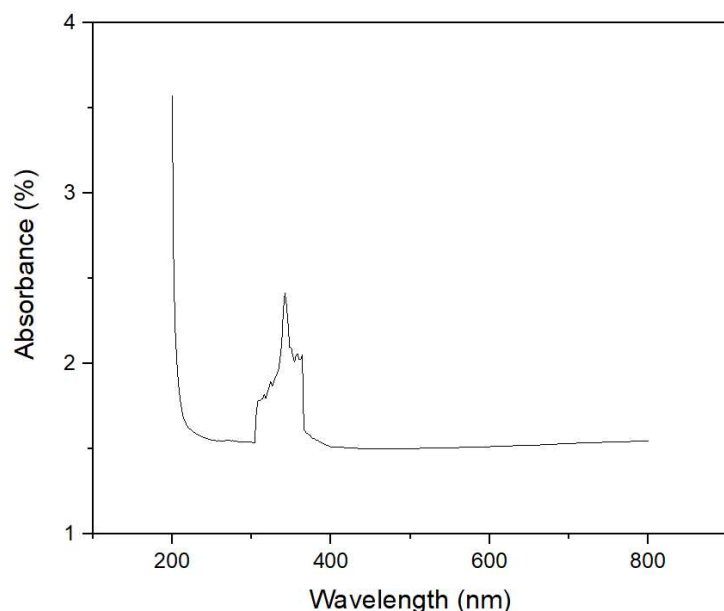


Figure.3.3. Absorbance spectra of pure tin oxide nanoparticles synthesized by precipitation method

The optical band gap of the material can be calculated from the absorption spectra using **Tauc equation**,

$$\alpha h\nu = D (h\nu - E_g)^n$$

Where α is the absorption coefficient of the prepared tin oxide nano powder, h is Planck's constant, ν is the frequency, D is a constant, E_g is the optical bandgap of the material and the exponent represents the type of optical transitions occurring in the prepared materials. The absorption coefficient α can be calculated using the following relation:

$$\alpha = 2.303A/t$$

Here, A represents the absorbance, and t is the width of the cuvette used for measuring the absorbance of the prepared material. Figure.11 shows the optical band gap of pure SnO₂ nano powder prepared and it is found to be 3.4eV. This value represents the energy difference between the highest occupied energy level (valence band) and the lowest unoccupied energy level (conduction band) in the material. The optical band gap of the tin oxide nano powder, as determined from the figure by extrapolating a linear fit to the photon energy axis with $\alpha = 0$ on the Y-axis, is 3.4eV. Interestingly, the obtained band gap value of 3.4eV aligns well with previously reported values.

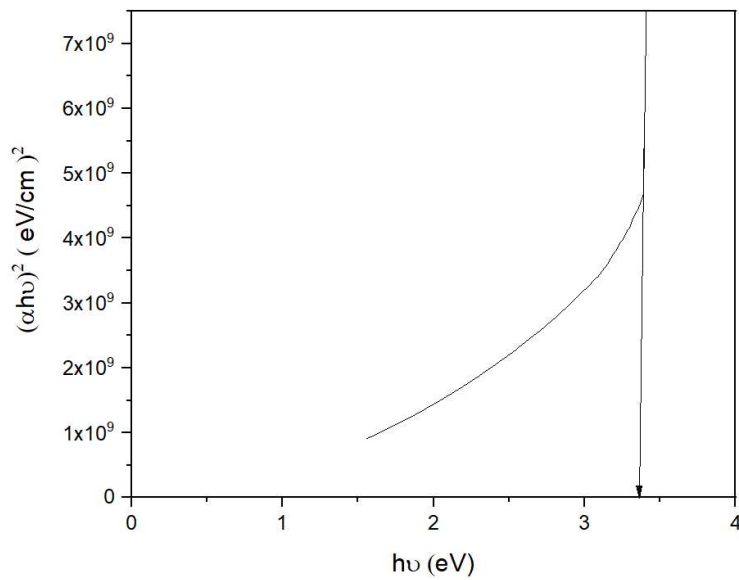


Figure 3.4. Optical bandgap of the pure tin oxide nanoparticles synthesized by precipitation method

3.1.4. Scanning Electron Microscopy (SEM)

The SEM image of pure SnO₂ nano particle prepared by precipitation method is given below. A Scanning Electron Microscope is type of electron microscope that scan the surface of the microorganisms using a beam of low energy electron to focus and examine specimen. The image was captured at a magnification of 10μm, 5μm, 1μm.

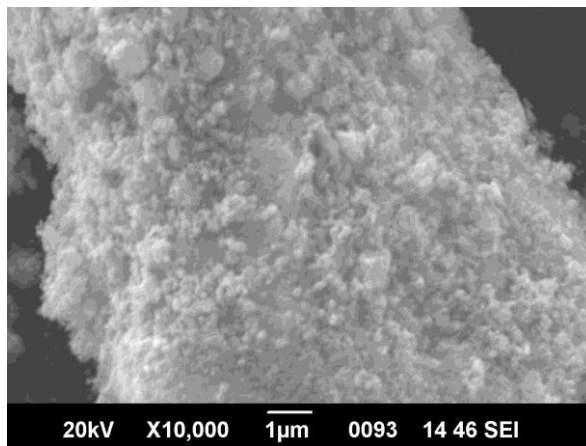
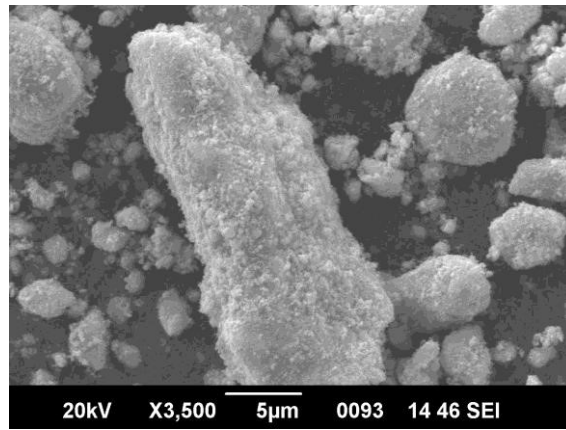
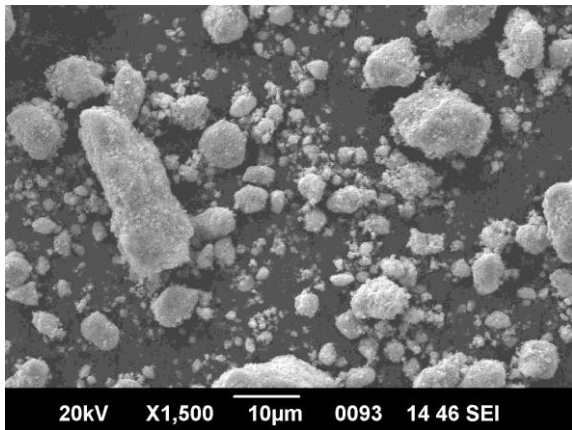


Figure.3.5.SEM image of pure SnO₂ synthesised by precipitation method

From figure we can observe granular grains and The micrograph shows the particle has irregular structure, to get particle size we have to take TEM analysis.

3.1.4. Photocatalytic activity of Tin oxide nano particle synthesized using precipitation method

The photocatalytic activity of the pure Tin oxide (SnO₂) nano particle over the methyl orange dye was evaluated by monitoring the optical absorption spectra of methyl orange solution under irradiation of direct sunlight and in the absence of sunlight. The degradation percentage of the methyl orange dye was calculated using the formula,

$$\text{Degradation percentage} = \left[\frac{A_0 - A_t}{A_0} \right] \times 100$$

Where,

A₀ is the absorbance of dye solution after 24 hour

A_t is the absorbance of dye solution after 48 hour

The figure given below shows the Photocatalytic degradation of methyl orange dye under the sunlight irradiation using SnO₂ nano particle.

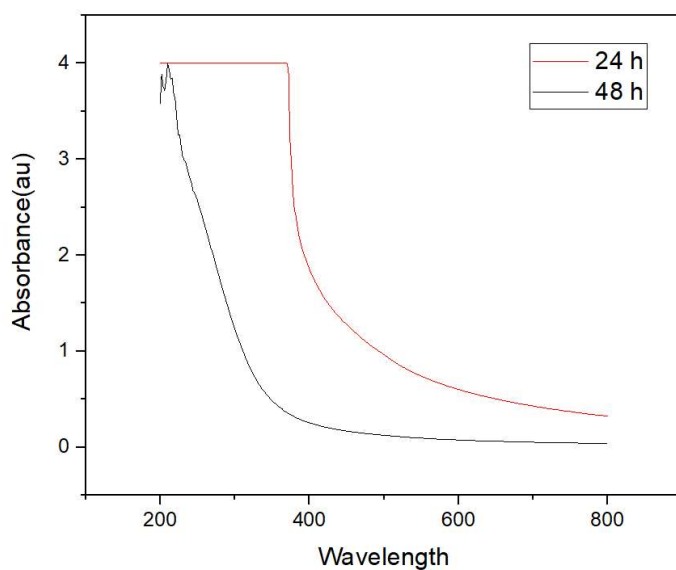


Figure.3.6. Photocatalytic degradation of methyl orange dye under the irradiation of direct sunlight using SnO₂ NPs

It was observed that degradation percentage of methyl orange dye using SnO₂ NPs is found to be 86.77%.

Where ,

$$A_0 = 0.31 \quad A_t = 0.041$$

$$\text{Absorption Percentage} = \frac{0.31 - 0.041}{0.31} \times 100 = 86.77\%$$

It shows that the prepared SnO₂ nano particle degraded methyl orange almost completely with in 48 hour.

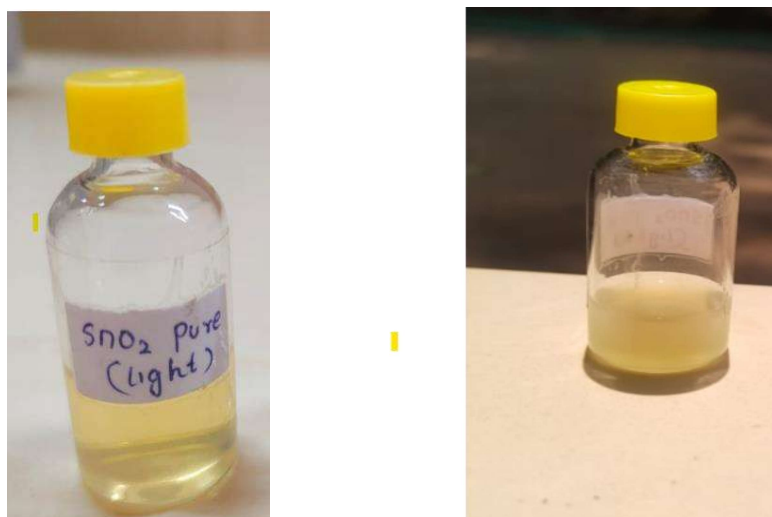


Figure.3.7. Methyl orange solution with SnO₂ NPs after 24 hour and after 48 hour placed under irradiation of direct sunlight

The figure given below shows the absorption spectra of photocatalytic action of Tin Oxide nanoparticle after 24 and 48 hour placed in dark place. The rate of degradation is calculated from the absorption spectra.

Where ,

$$A_0 = 0.14 \quad A_t = 0.050$$

$$\text{Absorption Percentage} = \frac{0.14 - 0.050}{0.14} \times 100 = 64.28\%$$

From the calculation, it is found that 64.28% of methyl orange dye was degraded with in 48 hour.

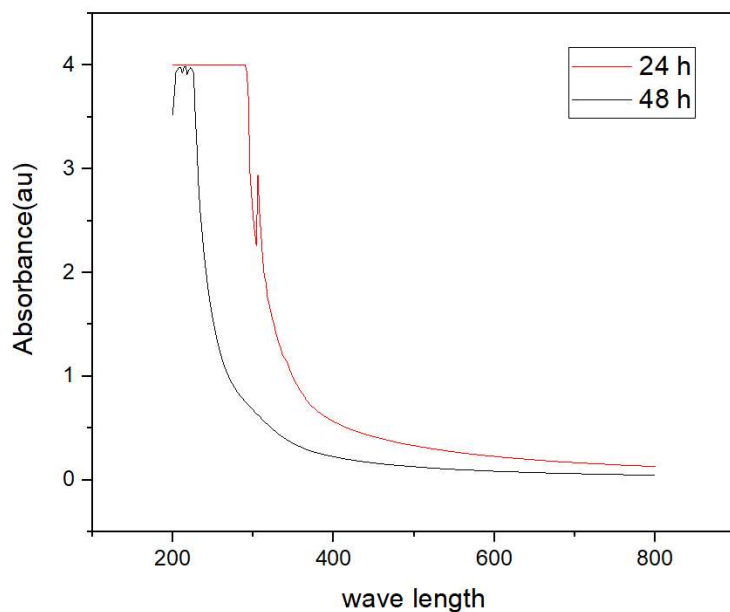


Figure.3.8. Photocatalytic degradation of methyl orange dye in absence of sun light using SnO₂ NPs

These two results shows that the Prepared SnO₂ NPs exhibited an outstanding photocatalytic degradation of methyl orange within 48 hour under presence of sunlight and also in the absence of

sunlight(dark).From these we can say that the synthesized SnO₂ nano particles can use effectively as a catalyst in degrading the organic dye such methyl orange and also other toxic organic compounds.

3.2. SYNTHESIS OF IRON DOPED SnO₂ NANOPOWDER

3.2.1.XRD analysis

The figure.8 shows the X-ray diffraction pattern of the Iron doped SnO₂ synthesized at calcination temperature 370 0°C.The peaks at 2θ value 26.564°, 33.8°, 51.8°and 54.6° correspond to the crystallographic planes (110), (101), (200), (211), and (220), respectively. All the peaks in XRD were matched with the diffraction data of the tetragonal structure of tin oxide. The spectra were plotted using the origin lab 2018. The particle size found using the Debye–Scherrer formula, which is determined to be 8.4972 nm.

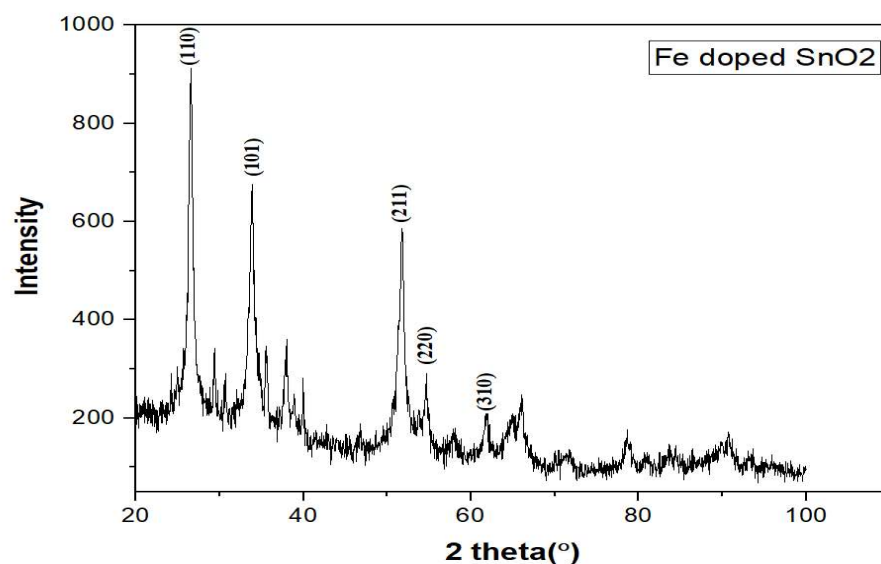


Figure.3.9. XRD of the Fe doped SnO₂ synthesized with calcination temperature 370°C

3.2.1(a).Crystalline size

In the case of Iron doped SnO₂ the grain size calculated using the Scherrer equation is found to be 8.603 nm.

For calcination Temperature 370 °C:-

XRD peaks Position 2θ (deg)	FWHM (β)	Bragg's peaks	Crystalline size D (nm)	Average crystalline size D (nm)
26.564	0.869	1 1 0	8.8973	8.4972
33.866	0.913	1 0 1	8.3240	
51.774	0.869	2 1 1	8.2245	
54.687	0.826	2 2 0	8.5431	

Table 3.6 Crystalline size of Fe doped SnO₂ calculated using Debye Scherrer's Equation

3.2.1(b).d interplanar spacing

The interplanar spacing of Iron doped SnO₂ is Calculated using the Braggs equation is shown below,

2 theta	Theta	d-spacing
26.5	13.25	3.3503
33.8	16.9	2.6441
37.9	18.95	2.3690
51.7	25.85	1.7644
54.7	27.35	1.6751
		This is our desire value i in Å

Table.3.7.d spacing of Fe doped SnO₂ calculated using Bragg's equation.

3.2.1.(c) WH Plot

To calculate crystalline size and strain of iron doped SnO₂ from XRD data we use Williamson-Hall (W-H) plot method. The plot of $(4 \sin \theta)$ on x-axis and $(\beta_T \cos \theta)$ on y-axis is shown below.

Theta (degree)	theta (radians)	FWHM (degree)	FWHM (radians)	$\beta \cos \theta$	$2 \sin \theta$
13.282	0.2318	0.869	0.015167	0.014761	0.45948
16.933	0.2955	0.913	0.015935	0.015244	0.582506
17.933	0.31299	0.869	0.015167	0.014440	0.615809
25.8435	0.4510	0.869	0.015167	0.01365	0.87182
27.3865	0.4779	0.826	0.014416	0.012801	0.91998

Table 3.8 values of $\beta \cos \theta$ and $4 \sin \theta$ for Fe doped SnO₂.

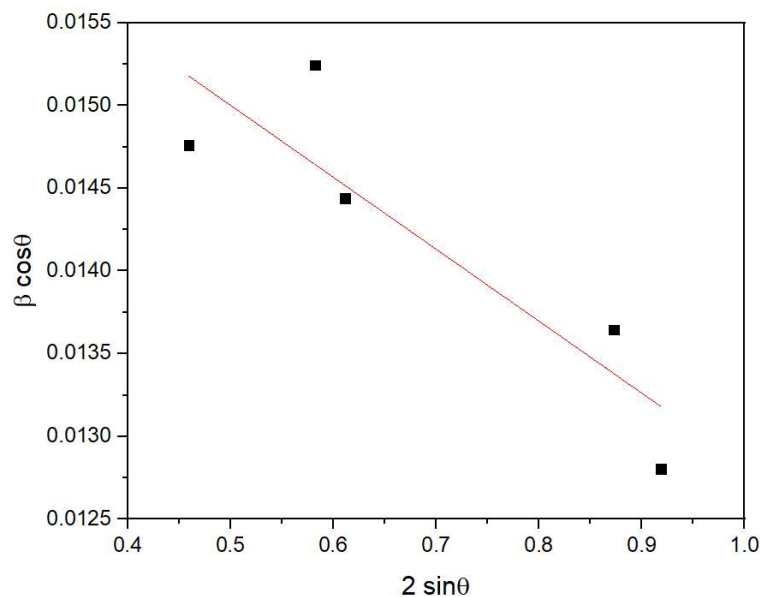


Figure 3.10 To calculate crystalline size and strain of Fe doped SnO₂ from XRD data using Williamson-Hall (W-H) plot method.

Slope of the plot is the strain. So the value of strain (ϵ) = -0.00435

The value of y-intercept “c” = 0.01717

$$\text{y-intercept } C = \frac{K\lambda}{D}$$

Or

$$D = \frac{k\lambda}{C}$$

Where $k = 0.9$ is the shape factor and $\lambda = 0.15418\text{nm}$ is the wavelength of the X-ray source, putting all these values we get,

$$D = 8.0753 \text{ nm}$$

In the case of Iron doped SnO₂ dislocation density can be calculated from the grain size as follows,

Grain Size (D) from the Scherrer's formula (nm)	Dislocation density ($\times 10^{15}$) (lines/m ²)	Grain size (D) from the W-H plot (nm)	Lattice strain
8.4972	13.8499	8.0753	-0.00435

Table.3.11. Grain size comparison data from Debye Scherrer's formula and W-H plot of Fe doped SnO₂

The texture coefficient in the case of Iron doped SnO₂ calculated using the equation

$$TC(hkl) = \frac{I(hkl)}{\frac{1}{N}\sum I(hkl)}$$

Where $TC(hkl)$ is the texture coefficient of hkl plane, $I(hkl)$ represents the intensity of the diffraction peak corresponding to the crystallographic plane (hkl).and N is the number of reflections.

hkl value	TC of Pure SnO ₂
1 1 0	1.479
1 0 1	1.09
2 0 0	0.95
2 1 1	0.47

Table 3.12 Texture coefficient of each (hkl) plane for doped SnO₂.

From the table 3.10, it is evident that (110) has high Texture coefficient, it indicate, it has high preferential orientation.

3.2.2.UV-VIS Spectroscopic Analysis

The UV-VIS spectroscopy of Fe doped SnO₂ was done at room temperature with in wavelength range 200nm-800nm.The Absorption spectrum of Fe doped SnO₂ synthesized by precipitation method at calcination temperature 370°C is given below.

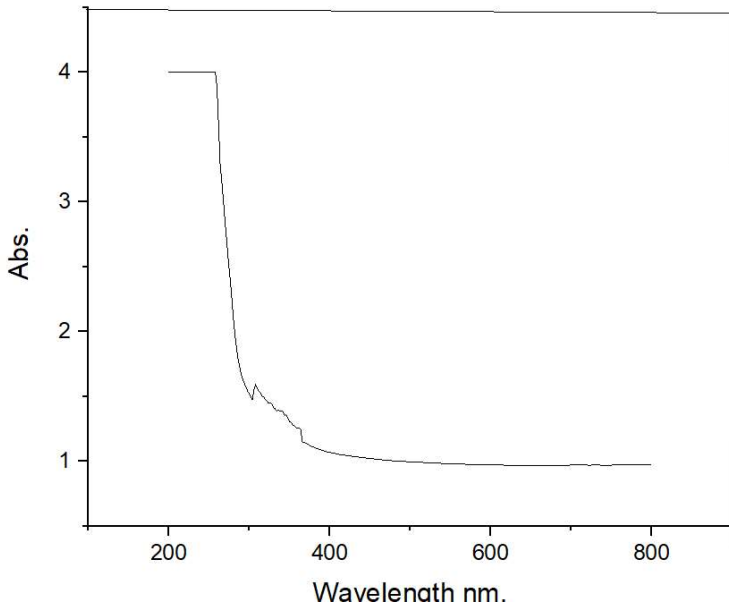
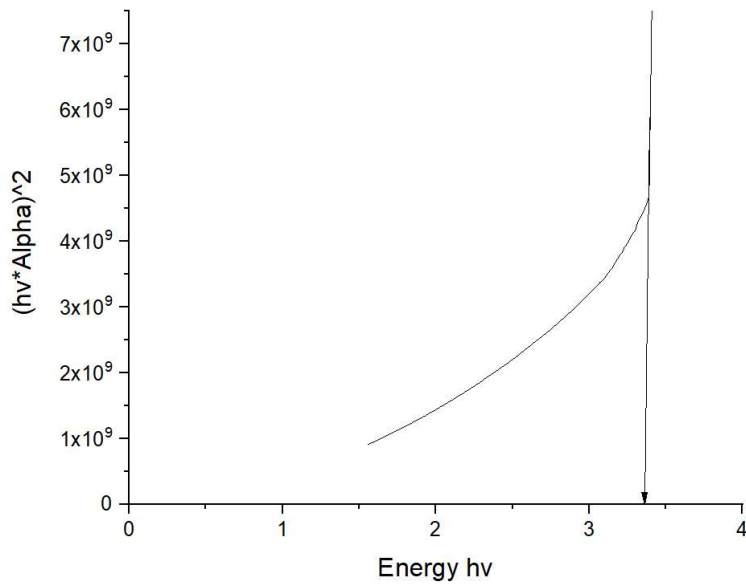


Figure.3.11. Absorbance spectra of Fe doped tin oxide nanoparticles synthesized by precipitation method

Figure.3.9 shows the optical band gap of pure SnO₂ nano powder prepared and it is found to be 3.4eV. The optical band gap of the Iron doped tin oxide nano powder, as determined from the figure by extrapolating a linear fit to the photon energy axis with $\alpha = 0$ on the Y-axis, is 3.34eV. Interestingly, the obtained band gap value of 3.43 eV aligns well with previously reported values.



Figur3.12.Optical bandgap Fe doped tin oxide nanoparticles synthesized by precipitation method

3.2.3. Scanning electron microscopy (SEM)

The SEM image of Iron doped SnO₂ nano particle prepared by precipitation method is given below. The image was captured at the magnification of 10 μ m, 5 μ m and 1 μ m.

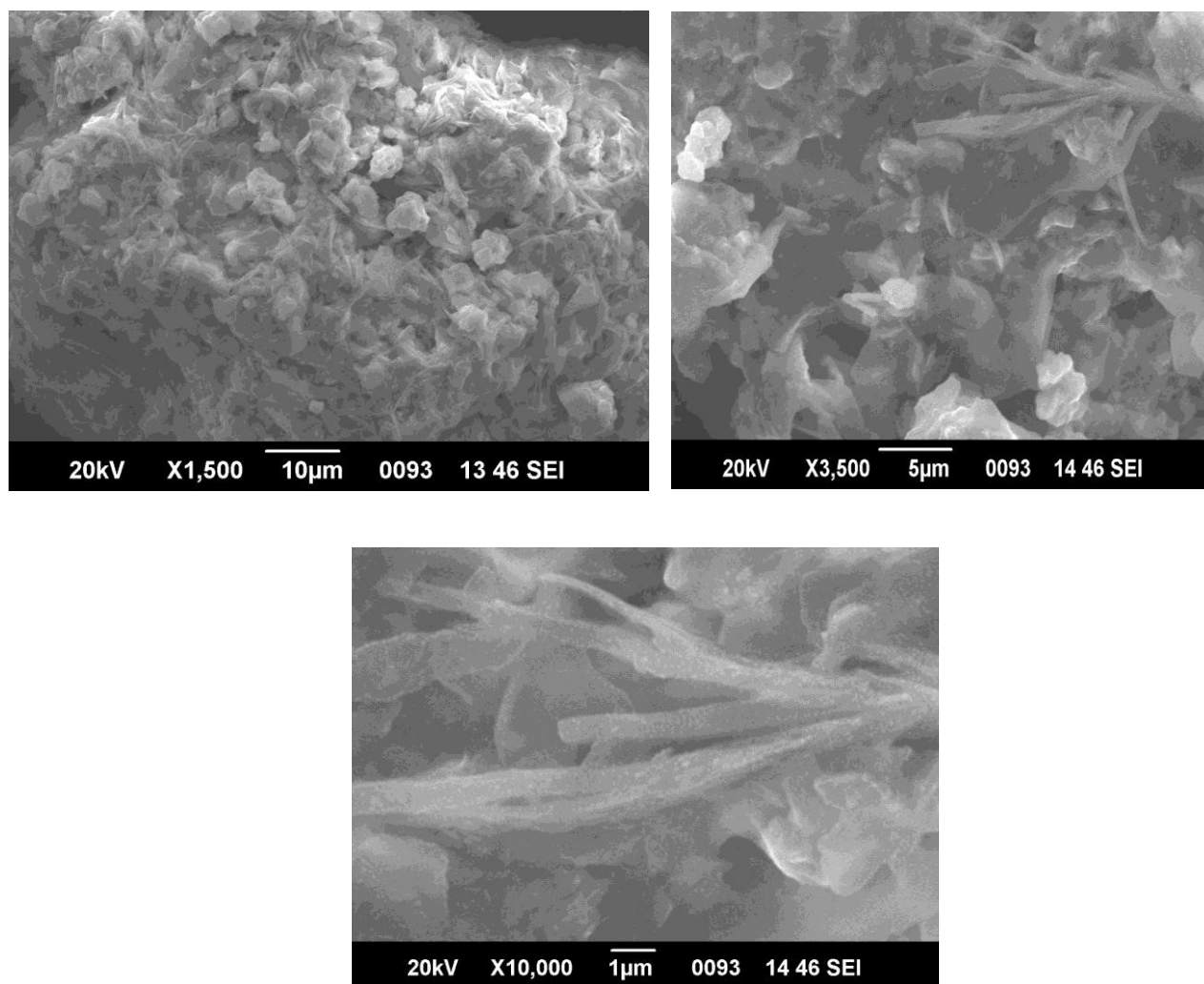


Figure.3.13. SEM image of Fe doped SnO₂ synthesised using precipitation method.

SEM image reveals that the particle has a homogeneous morphology, and nano tubes are formed.

3.3. Conclusion

SnO₂ nano powder was prepared successfully by preprecipitation method and the sample is analysed using different techniques like XRD, UV, SEM. The optical band gap was determined using the Tauc plot, resulting in an obtained value of 3.4 eV in the case of pure SnO₂ nano powder and 3.34 in the case of Fe doped SnO₂ nano powder. The XRD spectrum reveals that the prepared tin oxide nano powder has tetragonal structure, with an average crystallite size of approximately 12.5998nm for pure SnO₂ nano powder and 8.4972 for Fe doped SnO₂ nano powder. The calculated interplanar spacings from X-ray diffraction (XRD) data are as follows: 3.3498, 2.6460, 2.3690, 1.7644, 1.6748 and in the case of Fe doped SnO₂ it is found to be 3.3503, 2.6441, 2.3690, 1.7644, 1.6751. The strain and y-intercept calculated from the WH plot for pure SnO₂ nano powder is -0.00326 and 0.01202 and the grain size corresponding to this is 11.5442. The strain and y- intercept from WH plot in the case of Fe doped SnO₂ is -0.00435 and 0.01717 with corresponding grain size 8.0753. The photocatalytic activity of prepared tin oxide over the methyl orange dye was evaluated by calculating the rate of degradation. Absorption percentage is 86.77% for solution placed in direct sunlight and 64.28% for solution placed in dark place.

3.4.Future Scope of SnO₂ nano particle

SnO₂ has been largely investigated and used due its varieties of applications such as photocatalysis, gas sensing, lithium ion batteries, solar cells etc. The application mainly depends on their morphologies and special assemblies of nanomaterials. Tin oxide nanomaterials exhibit strong catalytic activity in the degradation of the organic pollutants in solutions because of their wonderful properties such as low cost, transparency, high photosensitivity, photostability etc. Its Gas sensing technology has garnered significant interest in practical applications, spanning both industrial and academic domains. The gas sensing means discriminating and monitoring the concentration of gases in the industrial processes as well as in everyday life. Due to high demand for reliable and robust gas sensing devices, academic research play important rule for improving the capability to detect the gas species. excellent electrical and optical property makes SnO₂ as suitable for gas sensing. It is also used in Lithium Ion batteries and solar cells.

